Vertical Structure and Microphysics analysis from events of heavy rainfall in Southeast of Brazil through polarimetric weather radars

Eliana Gatti[1], Izabelly Carvalho da Costa[2], Daniel Alejandro Vila[3] & Vinicius Banda Sperling[4]

[1] Instituto Nacional de Pesquisas Espaciais/INPE, Programa de Pós-Graduação em Meteorologia, Cachoeira Paulista/SP, Brasil. CEP: 12630-000.

[2] Instituto Nacional de Pesquisas Espaciais/INPE, Coordenação Geral de Ciências da Terra/CGCT, Cachoeira Paulista/SP, Brasil. CEP: 12630-000.

[3] Instituto Nacional de Pesquisas Espaciais/INPE, Coordenação Geral de Ciências da Terra/CGCT, São José dos Campos/SP, Brasil. CEP: 12227-010.

[4] Centro Nacional de Monitoramento e Alertas de Desastres Naturais/ CEMADEN, São José dos Campos/SP, Brasil. CEP: 12227-010.

eligatti12@gmail.com[1], izabelly.costa@inpe.br[2], daniel.vila@inpe.br[3], vini.meteorologia@gmail.com[4]
Gratuidade foto: Eliana Gatti

Abstract

The main objective of this study is to evaluate the vertical structure and the life cycle of the vertically integrated liquid (VIL) and ice (VII) content of seven cases of heavy rainfall using two polarimetric radars. The selected events accumulated more than 40 mm/h and occurred in the Southeast of Brazil between 2019-2020 The rainfall events were selected from rain gauges and validated with the radar data. During the life cycle of precipitation systems, VIL and VII were evaluated using the most intense reflectivity profile. We calculated the Contoured Frequency by Altitude Diagrams (CFAD) of Reflectivity and Differential Reflectivity (Zdr) to analyze the vertical structure and microphysics of the rain events. The results show that for the rain events generated by isolated storms, the life cycles of VIL and VII show more clearly the moment of convection enhancement, in which raindrops and ice grow inside the cloud, unlike what was observed in large precipitating systems. The CFADs diagram showed a higher frequency of radar reflectivity between 45 to 50 dBZ up to 6km. In addition, at 10 minutes before the peak of the event, an intensification of the updraft and greater ice formation at high levels occurred, followed by an increase in the frequency of positive Zdr values at low levels, indicating the start of precipitation. When compared to the literature, these results show certain differences between the cases of heavy rain and hail.

Keywords: Meteorology, mesoscale, extreme events.

Resumo

O principal objetivo deste estudo é avaliar a estrutura vertical e o ciclo de vida do conteúdo de água integrado verticalmente (VIL) e gelo (VII) de eventos de chuvas intensas usando dois radares polarimétricos. Os eventos selecionados acumularam mais de 40 mm/h e ocorreram no Sudeste do Brasil entre 2019-2020. Todos os eventos foram selecionados a partir de pluviômetros do Instituto Nacional de Meteorologia e validados com os dados dos radares. Durante o ciclo de vida dos sistemas que geraram a precipitação, o VIL e VII foram calculados utilizando o perfil de refletividade mais intenso. Para analisar a estrutura vertical e a microfísica dos eventos de chuva, diagramas de frequência (CFAD) das variáveis Refletividade e Refletividade Diferencial (Zdr) foram calculados. Os resultados mostram que para os eventos de chuva gerados por tempestades isoladas, os ciclos de vida de VIL e VII mostram mais claramente o momento de intensificação da convecção, em que gotas de chuva e o conteúdo de gelo crescem dentro da nuvem, ao contrário do que foi observado em grandes sistemas precipitantes. O diagrama CFAD mostrou uma maior frequência de refletividade do radar entre 45 a 50 dBZ até 6km. Além disso, 10 minutos antes do pico do evento, ocorreu uma intensificação da corrente ascendente e maior formação de gelo em níveis elevados, seguido por um aumento na frequência de valores Zdr positivos em níveis baixos, indicando o início da precipitação. Quando comparados à literatura, tais resultados mostram certas diferenças entre os casos de chuva intensa e granizo.

Palavras-Chave: Meteorologia; mesoescala, eventos extremos.

Resume

El objetivo principal de este estudio es evaluar la estructura vertical y el ciclo de vida del agua integrada verticalmente (VIL) y el contenido de hielo (VII) de eventos de fuertes lluvias

utilizando dos radares polarimétricos. Los eventos seleccionados acumularon más de 40 mm / hy tuvieron lugar en el sureste de Brasil entre 2019-2020. Todos los eventos fueron seleccionados de pluviómetros y validados con datos de radar. Durante el ciclo de vida de los sistemas que generaron la precipitación, se calcularon VIL y VII utilizando el perfil de reflectividad más intenso. Para analizar la estructura vertical y microfísica de los eventos de lluvia, se calcularon diagramas de frecuencia (CFAD) de las variables de Reflectividad y Reflectividad Diferencial (Zdr). Los resultados muestran que para los eventos de lluvia generados por tormentas aisladas, los ciclos de vida de VIL y VII muestran con mayor claridad el momento de intensificación de la convección, contrário a lo observado en los grandes sistemas de precipitación. El diagrama CFAD mostró una frecuencia más altas de reflectividad del radar entre 45 y 50 dBZ hasta 6 km. Además, 10 minutos antes del pico del evento, hubo una mayor formación de hielo en niveles altos, seguida de un aumento en la frecuencia de valores positivos de Zdr en niveles bajos, lo que indica el início de la precipitación. Al compararlos con la literatura, estos resultados muestran ciertas diferencias entre los casos de lluvia intensa y granizo.
Palabras-Claves: Meteorología; mesoescala, eventos extremos.

Introduction

Brazil is a large country with a north-south extension of 4394 km. Thus, its five regions are distributed over a wide range of latitudes, extending from 5°N to 33°S, and consequently, each of them has a different climate, as shown in Alvares et al. (2013). To characterize the climate of a region, precipitation is one of the main variables used, which is generated by different meteorological systems that affect each area in particular.

A large part of the precipitation systems that define the annual rainfall of an area provide episodes of heavy or extreme rain. Depending on the region of Brazil, different convective systems generate this type of event, as shown by Machado et al (2014). In the literature, there are different methodologies to characterize heavy rain as it varies according to the availability of data and the purpose of each research. For example, studies such as Brooks & Stensrud (2000), Konrad (1997), Groisman et al. (2012) and Dolif & Nobre (2012) used fixed thresholds to characterize heavy rain events. In Brazil, Teixeira & Satyamurty (2007) define heavy rainfall as when the isoline of 50 mm involves a region of at least 10,000 km². On the other hand, Liebmann et al. (2001) considered an event of extreme rainfall for the São Paulo state, when daily precipitation exceeds a given percent of the climatological mean for that period. In addition, some studies evaluate heavy rain by percentiles, such as Groisman et al. (2001) and Lima et al. (2010).

Although there are different ways to analyze heavy rain, most studies on the subject consider precipitation on a daily scale. However, several events that are associated with flash floods occur in a shorter period. They adversely affect urban populations because the infrastructure is often inadequate to accommodate flooding caused by these events (Liebmann et al., 2001). In Brazil, studies about heavy rain on a sub-daily scale are scarce. Thus, this work aims to evaluate some characteristics and verify if there is any common feature between them.

The understanding of the microphysical structure of precipitation in the absence of in situ measurements and the microphysical processes within the observed precipitation was improved using weather radars with dual-polarization, or just polarimetric (Murphy et al., 2020). This radar emits and receives electromagnetic waves oriented in both horizontal and vertical directions, providing a set of new variables capable of measuring different parameters compared to single-polarization radars (Zhao et al., 2019). Over the last ten years, Brazil has increased the polarimetric radar network, nonetheless, most are still single-polarized as even the complete network is not yet capable of covering the entire country. Thus, we highlight the importance of developing studies involving polarimetric radars in Brazil.

In this context, the main objective of this study is to evaluate the vertical structure and the life cycle of the Vertically Integrated Liquid (VIL) and Ice (VII) content of heavy rain events in the Southeast of Brazil from hourly precipitation observations using two polarimetric radars.

Data and Methodology

Study Area

The Southeast region of Brazil is annually affected by several meteorological systems that generate heavy rainfall and result in flash floods and various problems for population, such as cold fronts and the South Atlantic Convergence Zone. Thus, we selected two polarimetric radars from the National Center for Monitoring and Alerting of Natural Disasters (CEMADEN, in Portuguese) that cover part of the region, as shown in (Fig. 1).

Event Selection

We used two S-band radars both located in the Southeast region of Brazil, as shown in

(Fig. 1). They have dual-polarization and data availability every 10 minutes. The volumetric data were converted to CAPPI (Constant Altitude Plan Position Indicator) using the Radar Software Library (RSL) from NASA TRMM Satellite Validation Office. The CAPPI is a radar display which gives a horizontal cross-section of data at a constant altitude. Thus, we used CAPPI from 2 to 16 km high, providing 15 vertical levels.

The rain data used in this study come from automatic rain gauges from the National Institute of Meteorology (INMET, in Portuguese) with hourly frequency.

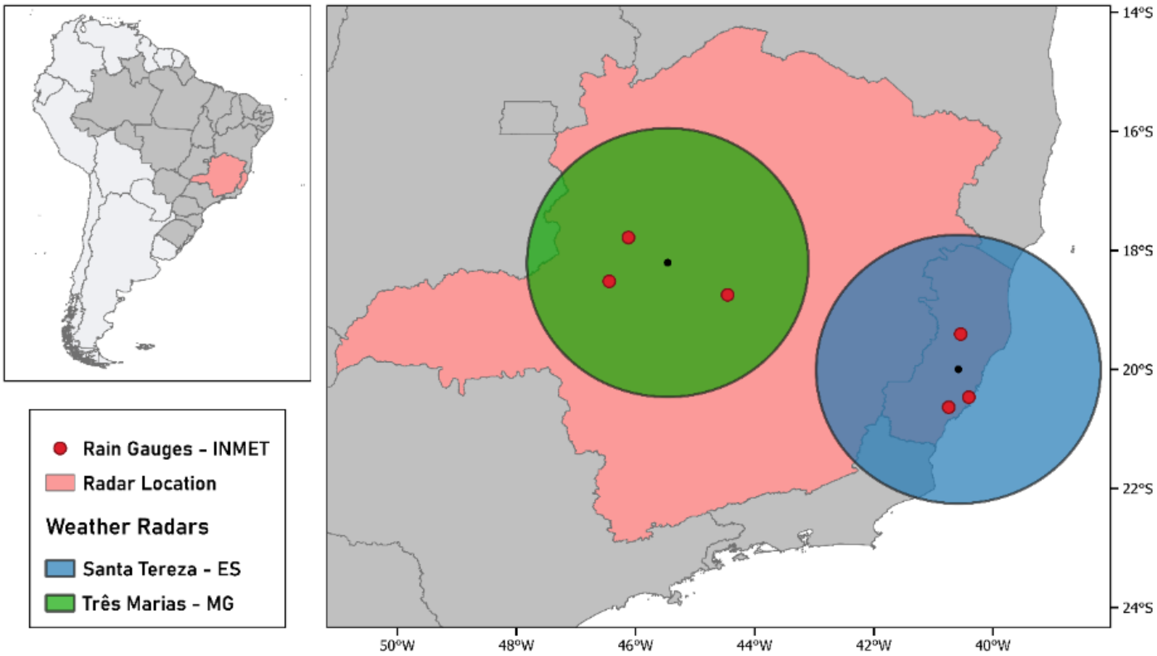

Figure 1 - Location of the Santa Tereza (blue) and Três Marias (green) polarimetric radars and the rain gauges selected for the study.

For the event selection, we filter the rain gauges between 50 and 150 km away from the centers of S-Band radars, to avoid the influence of the "cone of silence" (an area where there is no radar data) and possible effects of the Earth's curvature. After that, six rain gauges were selected, as shown in (Fig. 1). In this study it was considered heavy rainfall events if they presented accumulated rain precipitation greater than 40 mm/h between 2019 and 2020. To validate them, we used the CAPPI at 3 km. If at any time a reflectivity greater than or equal to 35 dBZ was registered above the gauge location, we selected the event. As a result, seven events are effectively used in this work.

Tracking

From a fixed reflectivity value, we tracked the systems that generated the events through an open-source software called TATHU (Tracking and Analysis of Thunderstorms) used operationally at the National Institute for Space Research (INPE, Brazil). For each time of the system life, we extract the system's georeferenced shapefile to obtain the location of each cloud that generated the rainfall episode.

Life Cycle VIL and VII

As reviewed by Villarini & Krajewskiand (2010), different sources of uncertainty are related to precipitation estimates using single-polarization radars which include radar miscalibration, attenuation, ground clutter, and anomalous propagation, among others. As VIL is an integration of Estimation of Liquid Water Content (LWC), this influences the result of VIL. However, it is clear in the literature the benefits obtained in calculating these estimates when using some polarimetric variables, as shown in Zrnic & Ryzhkov (1996) and Ryzhkov & Giangrande (2005).

Thus, in this work, we calculate the LWC and the IWC (Ice Water Content) through the following formulations, proposed by Ryzhkov & Zrnic (2019) and Bukovcic et al. (2018), respectively.

$$LWC = 2.25\, {K_{DP}}^{0.723} \tag{1}$$

$$IWC = 0.71\, {K_{DP}}^{0.65} Z^{0.28} \tag{2}$$

where K_{DP} is in $deg\ km^{-1}$ and Z is in $mm^6 m^{-3}$. As VIL and VII (Vertically Integrated Ice) are column integrations of LWC and IWC,

$$VIL = \int_{h_b}^{h_t} 2.25\, {K_{DP}}^{0.723}\, dh \tag{3}$$

$$VII = \int_{h_{-10°C}}^{h_{-40°C}} 0.71\, {K_{DP}}^{0.65} Z^{0.28}\, dh \tag{4}$$

both VIL and VII are in $kg\ m^{-2}$. h_b and h_t are the height (meters) of the base and top of the precipitation column. dh is the height (in meters), $h_{-10°C}$ and $h_{-40°C}$ are the height (meters) of the isotherms of $-10°C$ and $-40°C$, respectively. We obtain these heights using the atmospheric sounding closest to the gauges of each event, available in the University of

Wyoming Department of Atmospheric Sciences Database.

Vertical Structure and Microphysics

We calculate the Countored Frequency by Altitude Diagram (CFAD) (Yuter & Houze Jr., 1995) for the variables Reflectivity (dBZ) and Differential Reflectivity (Zdr) to analyze the vertical structure and microphysics of the heavy rain events. The CFADs show the frequency of occurrence of some variable values at different heights. We evaluate the CFADs from 30 minutes before to 20 minutes after the time of maximum pixel value (to complete one hour of the life cycle), following the technique proposed by Sperling (2018). This value is the time that the maximum reflectivity value at 3 km was registered in the gauge location (henceforth called Pmax).

We used an area of 5x5 pixels (25km²) centered on the maximum VIL value of each event and extract the reflectivity and Zdr profiles from 2 to 16 km to calculate the CFAD. As we extracted 25 profiles for each event and seven events are analyzed, the CFADs were created with 175 reflectivity and Zdr profiles.

The variable Zdr [20] is defined as,

$$\mathrm{Z}_{DR} = 10 \log \frac{Z_{HH}}{Z_{VV}} \tag{5}$$

where Z_{HH} (Z_{VV}) is the horizontally (vertically) transmitted and received radar reflectivity.

Zdr is a variable based on the particle axis and therefore differs from reflectivity in that it is not sensitive to particle concentration (Yuter & Houze Jr., 1995). Because it is based on the axis of the particles, it provides positive (negative) values for particles that are spatially oriented horizontally (vertical) and close to zero for spherical particles (Kumjian, 2013; Straka et al., (2000)).

Results and Discussion

Life Cycle of VIL and VII

Fig. 2 presents the calculation for the seven rain events studied. In this work, we do not filter any specific type of system tracked. However, analyzing the life cycle and comparing it with the CAPPI images of each event (not shown), there are some differences and similarities between them.

As shown in (Fig. 2A, 2B, 2E, 2F), there is an abrupt increase in the VIL and VII in moments before the Pmax (dashed vertical line). Right after such increase, there is a sharp drop in values. This increase may be associated with convection development, in which raindrops and ice grow in the cloud, and consequently result in higher reflectivity values. When the precipitation begins, values of VIL and VII drop. Although these four events have a common feature (cells that developed in isolation), they have some particularities. The rain events of (Fig. 2A) and (Fig. 2B) started their life cycle as small isolated clusters, reached maturity, and soon dissipated. However, the event in (Fig. 2E) showed an increase (mainly in ice content) but remained at high values for almost an hour and, just then, decreased. Among the seven events studied here, this was the one with the highest accumulated rainfall values, with more than 100 mm in two hours. As the data provided by the rain gauges are hourly, this accumulation was recorded as having occurred in two hours. However, considering the time of Pmax, it is clear that they were observed at two consecutive times, at 23:50 UTC on 01/17/2021 and 00 UTC on the 18th, indicating a great chance that this accumulation of more than 100 mm has occurred in a short period. This information corroborates with the life cycle VIL and VII because after 00 UTC, the values start to decrease. In (Fig. 2F), there is an increase in the variables from 02:50 UTC followed by the time of Pmax and right after a fall. However, soon after, the life cycle shows a second peak in water and ice content. It occurred because during the mature stage of this cloud it split into two clusters, with the part responsible for recording the highest reflectivity value, reaching its maximum and dissipating. On the other hand, the other cluster intensified again, resulting in the second peak in the VIL and VII values.

The events in (Fig. 2C) and (Fig. 2D) were clusters embedded in larger precipitation systems, so in general, did not show large variations in their lifecycle. The main difference between them is that the first one, at a certain point, broke away from the larger system and had a peak of intensification. Finally, and similar to the previous ones, the event in (Fig. 2G) showed few variations in its life cycle. It was a small, localized, and non-displaced system that showed mostly constant reflectivity values. Its peak of VIL and VII does not corroborate with the Pmax instant, suggesting that the cloud generated constant precipitation, without high values in just one moment, but in one hour accumulated more than 40 mm.

CFADs

In (Fig. 3), the CFAD for the seven heavy rainfall events is shown. Overall, the vertical structure of the events did not have a very evident change during this period. However, we can highlight some features.

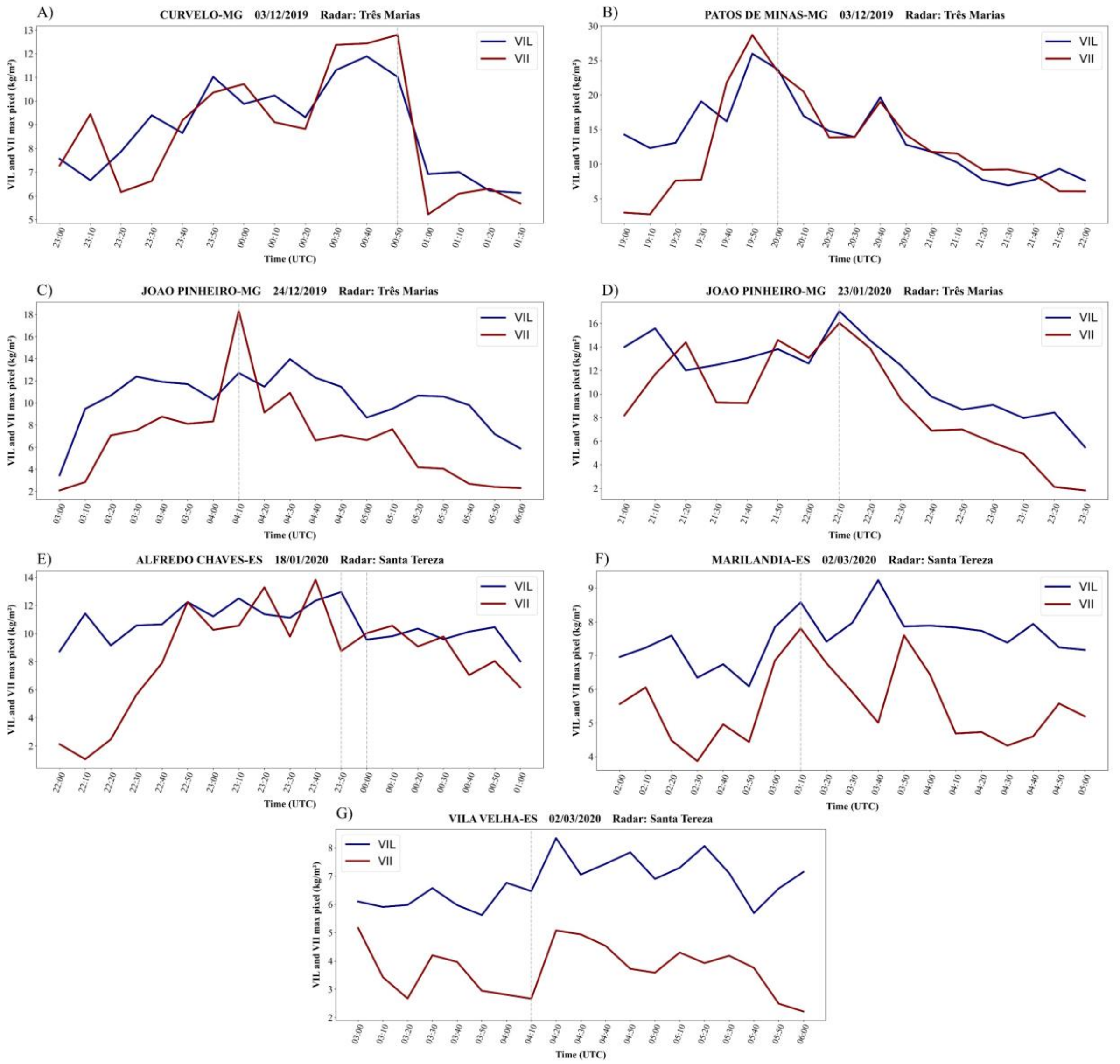

Figure 2. Vertically integrated liquid (VIL) and ice (VII) lifecycle for the highest value pixel for each analyzed event. The dashed vertical line indicates the time of maximum reflectivity value recorded by the rain gauge for each event, here called Pmax.

The highest frequency values occurred between the 45-50 dBZ range, extending from the cloud base to approximately 4km. At 10 minutes before the Pmax (-10 min), the frequency at higher heights increases, indicating the development of the updraft and the presence of ice, supporting the result showed at the Pmax instant, since the presence of ice in the cloud results from higher reflectivity values. At the instant of Pmax, the previously more structured column begins to decrease, possibly indicating the rain start time. In subsequent times, as there is no notable weakening, it is suggested that the rain, in general, did not occur in just one timestep, but rather, in a continuous manner. Sperling (2018) generated reflectivity CFADs for 16 hail cases that occurred in southern Brazil. Differently from the results obtained in this work, the study found the formation of a more intense convective column. Although, right after the hail reaches the surface, the convection quickly weakened.

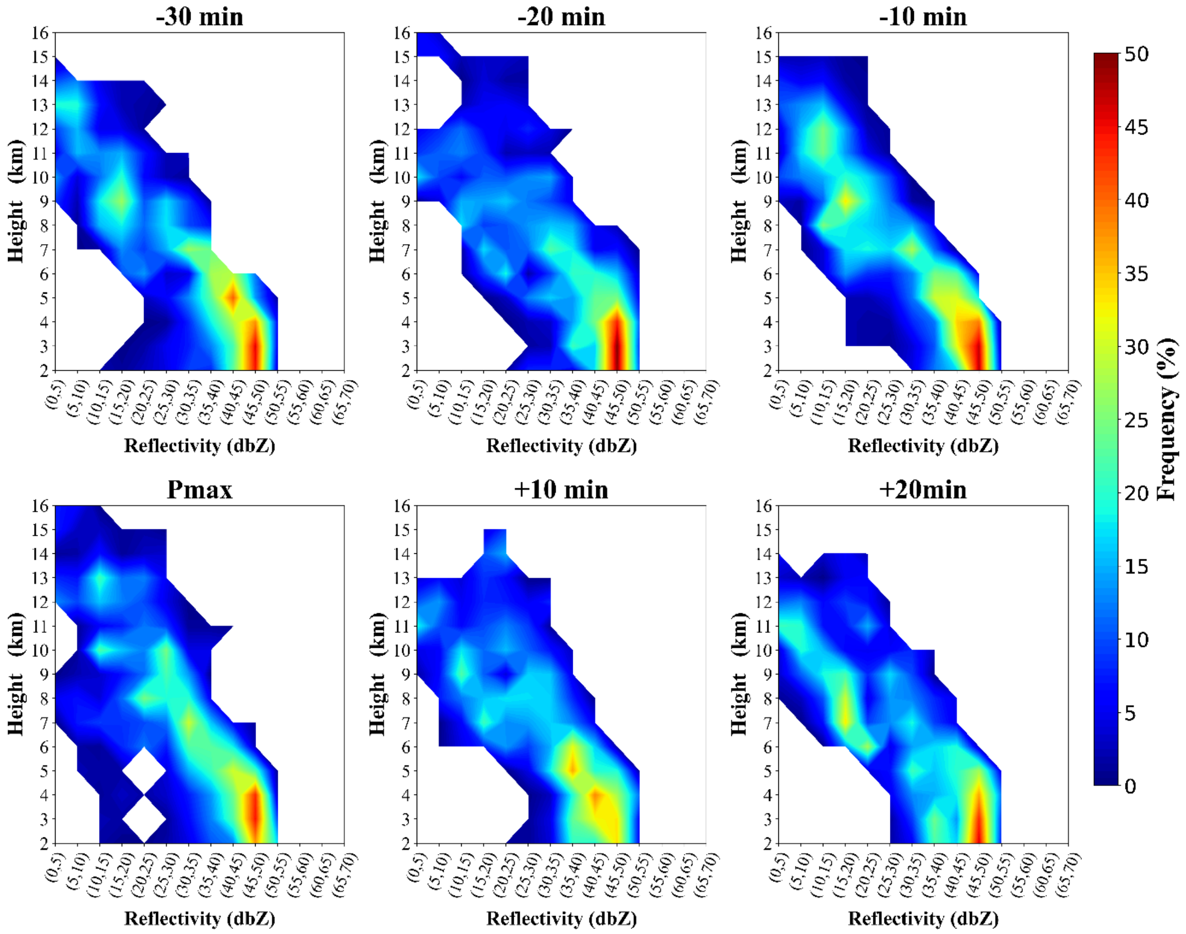

Figure 3. Frequency diagram (CFAD) using a 25 km² sample centered on the maximum VIL value for —30, —20, and —10 minutes before the occurrence of the maximum reflectivity value at the location of the rain gauge (Pmax), and +10, +20 minutes after registration. The y-axis refers to height in km and the x-axis to reflectivity intervals in dBZ.

The calculation of the CFAD for Zdr is shown in (Fig. 4). At the instants -30 min and -20 min, the highest frequency values obtained are between the intervals of 0 and 1, evincing the presence of spherical droplets in the lower areas of the cloud. In addition, although small, there are some frequency values between (2.5,3) intervals indicating that the cloud is in a growth phase. At the instant of -10min, the frequencies at the lower levels of the cloud decrease.

However, the column with higher frequency values develops. This increase in the Zdr column was also observed by Ryzhkov et al. (1994) and Kumjian et al. (2014). This occurs due a strengthening of the updraft carrying over the drops from the lower levels to the top of the cloud. Possibly some fractions of the droplets are frozen at higher levels, through processes like aggregation and accretion, resulting in a higher frequency of values in the range of negative values above 8 km, indicating ice formation. At the Pmax instant, the liquid drops fall inside the cloud and grow by processes such as collision and coalescence exhibiting the highest frequency values in positive intervals in the lower part of the cloud. It may be the approximate start time of rainfall. In subsequent times, the frequency loses intensity, however, the column remains with a very clear division of positive values of Zdr up to 6 km and negative values above. Due to the non-complete dissipation of the column and linking to the CFAD result in (Fig. 3), the rain, in general, occurred continuously after the cloud started the precipitation process.

.

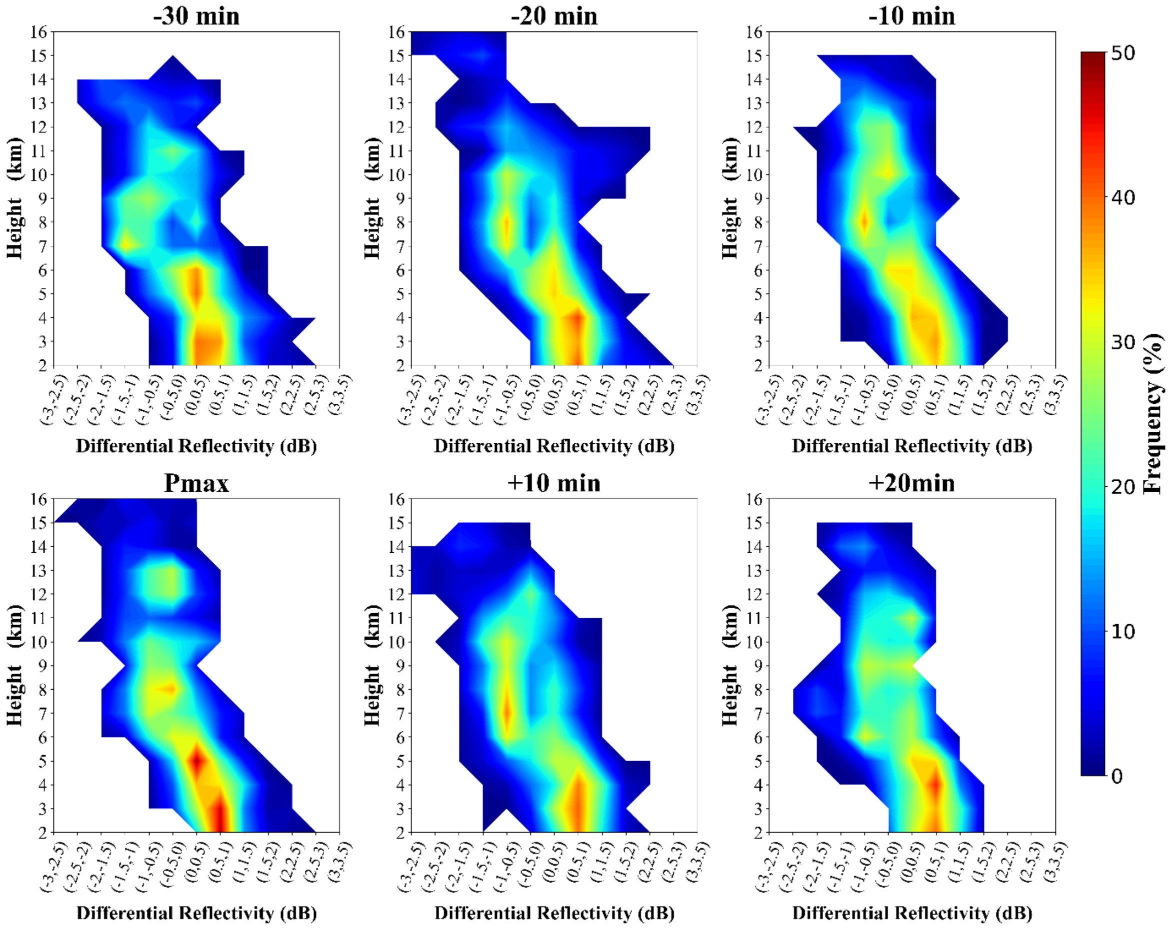

Figure 4. Same as Figure 3, but the x-axis refers to Differential Reflectivity (Zdr) values in dB.

Conclusions

As discussed, heavy rain events that occur in a short period are mainly responsible for flash floods that cause many disturbances to civilization. We investigated the behavior of seven heavy rain events occurred in the southeast region from Brazil to find out if there is any similarity between them and possibly increase their predictability.

Analyzing the VIL and VII life cycle, we concluded that the events generated by isolated storms present more evident characteristics of an abrupt increase in their water and ice content compared to events that belonged to a larger system. Comparing these results with radar images, these were the ones with the highest reflectivity values.

Concerning the vertical structure, at the instant before Pmax, the updraft developed. Minutes later, precipitation supposedly starts, due to high-frequency values of the positive Zdr intervals at low storm levels. It indicates that events occurred very quickly, which makes it difficult to issue alerts associated with this type of event in particular. In general, the results show characteristics found in convective clouds. However, heavy rain events presented reflectivity values between 45-50 dBZ at heights up to 6km, which are lower comparing severe convection events, such as those studied by Sperling (2018). It is still necessary to evaluate this type of event using a larger data sample to verify if this is a characteristic that differentiates them from other events generated by convective clouds.

In Brazil, there are not many published works that assess this type of rain event. With the inclusion of polarimetric radars, it became possible to evaluate some features that had not been explored yet. However, the polarimetric radar network is still scarce and does not have full coverage in the country, making it difficult to carry out work of national scope. Thus, future works need to be developed to show the efficiency of this set of new variables in the country, mainly to evaluate heavy rain events and make their prediction easier.

Acknowledgment

The first author thanks the National Council for Scientific and Technological Development (CNPq) for the Master's scholarship received in the PostGraduation Program in Meteorology at the Nacional Institute of Space Research (INPE).

References

Alvares et al. Köppen’s climate classification map for Brazil. Meteorologische Zeitschrift, Stuttgart, 22(6): 711-728, 2013.

Brooks HE, Stensrud DJ. Climatology of heavy rain events in the United States from hourly precipitation observations. Monthly Weather Review, American Meteorological Society, 128(4): 1194–1201, 2000.

Bukovcic P, Ryzhkov A, Zrnic D, Zhang G. Polarimetric radar relations for quantification of snow based on the disdrometer data. Journal of Applied Meteorology and Climatology, 57(1): 103–120, 2018.

Dolif G, Nobre C. Improving extreme precipitation forecasts in Rio de Janeiro, Brazil: are synoptic patterns efficient for distinguishing ordinary from heavy rainfall episodes? Atmospheric Science Letters, Wiley Online Library, 13(3): 216–222, 2012.

Groisman PY, Knight RW, Karl TR. Heavy precipitation and high streamflow in the contiguous United States: Trends in the twentieth century. Bulletin of the American Meteorological Society, American Meteorological Society, 82(2): 219–246, 2001.

Groisman PY, Knight RW, Karl TR. Changes in intense precipitation over the central united states. Journal of Hydrometeorology, 13(1): 47–66, 2012.

Konrad CE. Synoptic-scale features associated with warm season heavy rainfall over the interior southeastern United States. Weather and Forecasting, 12(3): 557–571, 1997.

Kumjian MR. Principles and applications of dual-polarization weather radar. part i: Description of the polarimetric radar. Journal of Operational Meteorology, 1, 2013.

Kumjian MR, Khain AP, Benmoshe N, Ilotoviz E, Ryzhkov AV, Phillips VT. The anatomy and physics of z dr columns: Investigating a polarimetric radar signature with a spectral bin microphysical model. Journal of Applied Meteorology and Climatology, 53(7): 1820–1843, 2014.

Liebmann B, Jones C, Carvalho LM. Interannual variability of daily extreme precipitation events in the state of Sao Paulo, Brazil. Journal of Climate, 14(2): 208–218, 2001.

Lima KC, Satyamurty P, Fernández JPR. Large-scale atmospheric conditions associated with heavy rainfall episodes in southeast Brazil. Theoretical and Applied Climatology, Springer, 101(1):121–135, 2010.

Machado LT, et al. The CHUVA project: How does convection vary across Brazil? Bulletin of the American Meteorological Society, 95(9): 1365-1380, 2014.

Murphy AM, Ryzhkov A, Zhang P. Columnar vertical profile (cvp) methodology for validating polarimetric radar retrievals in ice using in situ aircraft measurements. Journal of Atmospheric and Oceanic Technology, 37(9):1623–1642, 2020.

Ryzhkov AV, Zhuravlyov VB, Rybakova NA. Preliminary results of X-band polarization radar studies of clouds and precipitation. Journal of Atmospheric and Oceanic Technology, 11(1): 132-139, 1994.

Ryzhkov AV, Giangrande SE, Schuur TJ. Rainfall estimation with a polarimetric prototype of wsr-88d. Journal of Applied Meteorology, 44(4): 502–515, 2005.

Ryzhkov AV, Zrnic DS. 2019. Radar polarimetry for weather observations. Springer. 486p.

Seliga TA, Bringi V. Potential use of radar differential reflectivity measurements at orthogonal polarizations for measuring precipitation. Journal of Applied Meteorology and Climatology, 15(1):69-76, 1976.

Sperling VB. Processos Físicos e Elétricos das Tempestades de Granizo na Região Sul do Brasil. 2018. Tese (Doutorado em Meteorologia). Instituto Nacional de Pesquisas Espaciais (INPE). 211p.

Straka JM, Zrnic DS, Ryzhkov AV. Bulk hydrometeor classification and quantification using polarimetric radar data: Synthesis of relations. Journal of Applied Meteorology, 39(8): 1341-1372, 2000.

Teixeira MS, Satyamurty, P. Dynamical and synoptic characteristics of heavy rainfall episodes in southern brazil. Monthly Weather Review, American Meteorological Society, 135(2): 598-617, 2007.

Villarini G, Krajewski WF. Review of the different sources of uncertainty in single polarization radar-based estimates of rainfall. Surveys in Geophysics, Springer, 31(1): 107–129, 2010.

Yuter SE, Houze Jr. RA. Three-dimensional kinematic and microphysical evolution of Florida cumulonimbus. part ii: Frequency distributions of vertical velocity, reflectivity, and differential reflectivity. Monthly weather review, 123(7): 1941–1963, 1995.

Zhao K et al. Recent progress in dual-polarization radar research and applications in china. Advances in Atmospheric Sciences, Springer, 36(9): 961–974, 2019.

Zrnic D, Ryzhkov A. Advantages of rain measurements using specific differential phase. Journal of Atmospheric and Oceanic Technology, 13(2): 454–464, 1996.